Structures of Model Phosphinoamide Anions

Georges Trinquier[1] and Michael T. Ashby*[,2]

Laboratoire de Physique Quantique, IRSAMC-CNRS, Université Paul-Sabatier, 31062 Toulouse Cedex, France, and Department of Chemistry and Biochemistry, University of Oklahoma, 620 Parrington Oval, Norman, Oklahoma 73019

Received July 16, 1993®

Ab initio calculations have been carried out on the parent phosphinoamide/iminophosphide anion H_2PNH^- and all of its fluoro derivatives. The geometries, optimized at the SCF level, reveal two real minima related by a saddle point. The two minima correspond to cis and trans conformations, and the saddle point, in most cases, corresponds to the rotational barrier about the PN bond. The energies of the cis and trans forms of H_2PNH^-, $HFPNH^-$, and $HFPNF^-$ are degenerate within 1 kcal/mol at the MP4 level. The trans forms of H_2PNF^-, F_2PNH^-, and F_2PNF^- are unfavored relative to the cis forms by 4–6 kcal/mol. The transition states relating the two forms range from 8 kcal/mol for H_2PNH^- to 22 kcal/mol for $HFPNF^-$. The P—N bond in the parent anion H_2PNH^- is significantly shortened with respect to a regular single-bond length. This effect mainly originates from some delocalization of the nitrogen in-plane n_σ lone pair into the symmetrical combination of the empty PH σ^* orbitals. The hyperconjugation is not sufficient, however, to describe H_2PNH^- as an iminophosphide $H_2P^-{=}NH$; the system is best described as a phosphinoamide anion $H_2P{-}NH^-$ with the negative charge located mainly on nitrogen. Substitution of hydrogen for fluorine at phosphorus strengthens the P—N bond while substitution of hydrogen for fluorine at nitrogen weakens the P—N bond. The order of decreasing P—N bond strength is F_2PNH^-, $HFPNH^-$, F_2PNF^-, $HFPNF^-$, H_2PNH^-, H_2PNF^-, where F_2PNH^- is formally closest to an iminophosphide form. A model complex with lithium $[Li(H_2PNH)]_2$ has been investigated, and it does not exhibit the short P—Li contact that has been observed experimentally in $[Li(Ph_2PNPh)(OEt_2)]_2$.

The P—N bonds of phosphazanes $R_2P{-}NR'_2$ and phosphazenes $RP{=}NR'$ and their cyclic analogues have attracted the attention of experimentalists and theorists alike. Phosphazenes, because they possess formal P—N double bonds, exhibit comparatively short PN bond lengths.[3] Phosphazanes possess formal P—N single bonds, but they too can exhibit short PN bond lengths, especially when they bear σ-withdrawing substituents at phosphorus or when they exhibit trigonal planar geometry about their nitrogen atoms.[4] Other compounds may be cited that exhibit PN bond distances that fall between a single- and a double-bond length. Such is the case for aminophosphenium cations[5] $RPNR_2^+$ and phosphinoamide anions R_2PNR^-, a derivative of which was recently prepared by one of us.[6]

The ion Ph_2PNPh^- is synthesized from the corresponding aminophosphine Ph_2PNHPh by treatment with *n*-butyllithium.[6] Well-formed crystals of $[Li(Ph_2PNPh)(OEt_2)]_2$ precipitate when diethyl ether is used as a solvent. The solid-state structure of the $Li(Ph_2PNPh)$ moiety as determined by single-crystal X-ray crystallography consists of a centrosymmetric dimer, loosely held together by ion–dipole bonds that are typical of lithium salts.[7] Of particular interest with respect to the electronic structure of Ph_2PNPh^- is the relatively short P—N distance observed in $[Li(Ph_2PNPh)(OEt_2)]_2$ (1.672(2) Å), which suggests partial P—N multiple-bonding character. A direct comparison of the P—N bond length found for $[Li(Ph_2PNPh)(OEt_2)]_2$ to related bond lengths found in phosphazanes and phosphazenes is complicated by the apparent sensitivity of P—N bond lengths to substituent effects. Furthermore, there will likely be some influence of the Li—N and Li—P dipolar interactions on the P—N bond length. Nonetheless, it can be said that the P—N distance observed in $[Li(Ph_2PNPh)(OEt_2)]_2$ falls somewhere between the expected P—N single- and double-bond lengths.

The Ph_2PNPh^- ion has been described as a resonance hybrid of the phosphinoamide **1** and iminophosphide **2** anions.[6] Reso-

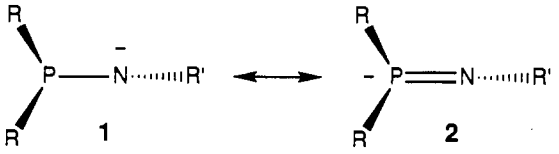

nance form **1** bears phosphorus(III) and a formal negative charge on the nitrogen atom, whereas resonance form **2** also bears phosphorus(III), but the formal negative charge is located on the phosphorus atom. Form **1** is expected to prevail if electronegativity is the dominate factor; however, form **2**, in which phosphorus has expanded its octet, results in additional stabilization due to resonance delocalization of the charge and P—N multiple bonding. The current explanation of the way phosphorus violates the octet rule involves electron-rich bonds or the hyperconjugation

* Abstract published in *Advance ACS Abstracts*, February 1, 1994.

(1) Université Paul-Sabatier.

(2) University of Oklahoma.

(3) (a) Tinquier, G. *J. Am. Chem. Soc.* **1982**, *104*, 6969. (b) Nguyen, M. T.; McGinn, M. A.; Hegarty, A. F. *J. Am. Chem. Soc.* **1985**, *107*, 8029. (c) Schmidt, M. W.; Gordon, M. S. *Inorg. Chem.* **1986**, *25*, 248. (d) Ito, K.; Nagase, S. *Chem. Phys. Lett.* **1986**, *126*, 531. (e) Nguyen, M. T.; Ha, T.-K. *Chem. Phys. Lett.* **1989**, *158*, 135. (f) Schoeller, W. W. In *Multiple Bonds and Low Coordination in Phosphorus Chemistry*; Regitz, M., Scherer, O. J., Eds.; Thieme Verlag: Stuttgart, Germany, 1990; p 5.

(4) For ab initio calculations on aminophosphine and derivatives see: (a) Cowley, A. H.; Mitchell, D. J.; Whangbo, M.-H.; Wolfe, S. *J. Am. Chem. Soc.* **1979**, *101*, 5224. (b) Gonbeau, D.; Liotard, D.; Pfister-Guillouzo, G. *Nouv. J. Chim.* **1980**, *4*, 228. (c) Barthelat, M.; Mathis, R.; Mathis, F. *J. Mol. Struct.* **1981**, *85*, 351. (d) Galasso, V. *J. Electron Spectrosc. Relat. Phenom.* **1983**, *32*, 359. (e) Magnusson, E. *J. Comput. Chem.* **1984**, *5*, 612. (f) Galasso, V. *J. Chem. Phys.* **1984**, *80*, 365. (g) Reed, A. E.; Schleyer, P. v. R. *Inorg. Chem.* **1988**, *27*, 3969. (h) Sudhakar, P. V.; Lammertsma, K. *J. Am. Chem. Soc.* **1991**, *113*, 1899.

(5) Marre, M.-R.; Trinquier, G. *J. Phys. Chem.* **1983**, *87*, 1903.

(6) Ashby, M. T.; Li, Z. *Inorg. Chem.* **1992**, *31*, 1321.

(7) (a) Fenton, D. E. In *Comprehensive Coordination Chemistry*; Wilkinson, G. Ed.; Pergamon Press: Oxford, 1987; Vol. 3, pp 1–80. (b) Setzer, W. N.; Schleyer, P. von R. *Adv. Organomet. Chem.* **1985**, *24*, 353.

0020-1669/94/1333-1306$04.50/0

Table 1. Geometrical Parameters (Å, deg)[a]

			P–N	P–H		P–F		N–H	N–F	XPY	PNZ	XPNZ	YPNZ
H_2P–NH^-	TS	C_1	1.657	1.449	1.460			1.012		100.2	110.7	35.1	130.4
	trans	C_s	1.649	1.447				1.013		100.0	105.4	132.3	132.3
	cis	C_s	1.638	1.463				1.015		99.1	112.6	48.3	48.3
HFP–NH^-	TS2	C_1	1.612	1.473		1.659		1.014		103.5	111.7	155.6	58.6
	TS1	C_1	1.601	1.461		1.697		1.008		102.1	118.2	22.0	118.7
	trans	C_1	1.604	1.429		1.713		1.013		100.0	107.2	102.7	163.4
	cis	C_1	1.595	1.454		1.717		1.014		98.5	113.6	61.9	32.4
H_2P–NF^-	TS	C_1	1.723	1.425	1.444				1.504	102.5	101.3	30.3	125.6
	trans	C_1	1.683	1.452	1.427				1.508	102.1	101.4	111.7	153.5
	trans	C_s	1.682	1.437					1.507	101.8	101.7	132.3	132.3
	cis	C_s	1.656	1.437					1.505	102.9	105.9	49.5	49.5
F_2P–NH^-	TS	C_1	1.570			1.675	1.650	1.008		104.1	116.8	138.3	40.5
	trans	C_s	1.574			1.654		1.011		99.3	106.8	133.3	133.3
	cis	C_s	1.562			1.677		1.014		98.6	115.7	47.0	47.0
HFP–NF^-	TS2	C_1	1.687	1.434		1.654			1.513	107.1	96.5	145.6	47.0
	TS1	C_1	1.689	1.452		1.639			1.462	104.2	106.9	18.2	116.1
	trans	C_1	1.629	1.420		1.692			1.483	102.2	104.0	98.8	168.0
	cis	C_1	1.617	1.424		1.681			1.473	111.2	109.0	65.7	30.7
F_2P–NF^-	TS	C_1	1.640			1.620	1.641		1.452	106.6	107.6	28.3	127.7
	trans	C_1	1.622			1.655	1.625		1.478	100.8	101.2	107.3	159.6
	trans	C_s	1.622			1.641			1.472	99.5	101.4	133.8	133.8
	cis	C_s	1.597			1.639			1.443	100.2	111.2	48.0	48.0

[a] TS stands for transition state. See **15** and **16** for the definition of TS1 and TS2.

mechanism. With few exceptions,[8] phosphorus d orbitals are not involved to a large extent in the bonding of such compounds.[9]

The present paper is a theoretical study of the model anions R_2PNR^-. Ab initio calculations have been performed to understand the geometric and electronic structure of the parent anion H_2PNH^- and its five fluoro derivatives. The fluoro substituents are expected to have a sizable effect on the strength and multiplicity of the P—N bond.[10] The geometries have been optimized at the SCF level, and the energies have been refined at a correlated level using fourth-order Moller–Plesset perturbation theory (MP4). After a short technical section, the parent anion H_2PNH^- and its complex with lithium cations $[Li(H_2PNH)]_2$ will be discussed first; then the fluoro derivatives of the anion will be covered. Throughout the paper, a parallel is drawn between the parent phosphinoamide anion H_2PNH^- and the parent aminophosphine $H_2P—NH_2$ and phosphazene HP=NH. The last two compounds were recalculated using our basis sets for the sake of consistency.

Method and Basis Sets

The calculations were performed with the HONDO8 program from the MOTECC89 package.[11] The core electrons were taken into account through a pseudopotential technique[12] for all of the atoms except hydrogen. The valence basis sets were of the double-ζ + polarization + diffuse type. The exponents for the d polarization functions on P, N, and F were 0.57, 0.95, and 0.90, respectively. The exponent for the p polarization function for H was 0.80. Because of the anionic nature of our systems, the double-ζ set was augmented by a set of diffuse s and p functions (s only for hydrogen) optimized on the atomic anions in their ground states. The exponents for the s diffuse functions for P, N, F, and H were 0.045, 0.063, 0.065, and 0.028, respectively. Those for the p diffuse functions for P, N, and F were 0.022, 0.056, and 0.079, respectively. The basis set for lithium that was used in the calculation of the model complex was of triple-ζ s and double-ζ p quality, with one of the s and p exponents chosen to correspond to a diffuse function. Our basis set can therefore be considered of triple-ζ + polarization quality. The optimized geometries were obtained using the analytical gradients. The final gradient cartesian components were less than 10^{-6}. The harmonic vibrational frequencies were obtained from force constants calculated by finite differences of analytical first derivatives. The zero-point energy corrections (ZPC) were calculated from zero-point energies (ZPE) scaled by a factor of 0.9.

Table 2. Relative Energies (kcal/mol)[a]

		SCF	MP4	MP4+ZPC
H_2P–NH^-	TS	7.4	7.9	7.1
	trans	0.7	0.5	0.6
	cis	0.0	0.0	0.0
HFP–NH^-	TS2	13.5	15.9	14.7
	TS1	12.1	14.4	13.3
	trans	0.1	0.0	0.0
	cis	0.0	0.2	0.5
H_2P–NF^-	TS	14.3	15.9	15.2
	trans	5.7	6.4	6.0
	cis	0.0	0.0	0.0
F_2P–NH^-	TS	9.7	9.8	8.9
	trans	3.6	3.7	3.7
	cis	0.0	0.0	0.0
HFP–NF^-	TS2	18.3	22.2	21.5
	TS1	26.5	32.3	31.5
	trans	1.5	1.0	1.0
	cis	0.0	0.0	0.0
F_2P–NF^-	TS	16.4	17.1	16.5
	trans	4.5	4.3	4.0
	cis	0.0	0.0	0.0

[a] ZPC stands for zero-point-energy corrections.

The Parent Anion H_2PNH^-

Exploration of the H_3PN^- potential surface led to two real minima of C_s symmetry: a cis form **3** and a trans form **4** of H_2PNH^-, related by a saddle point of index 1 of C_1 symmetry,

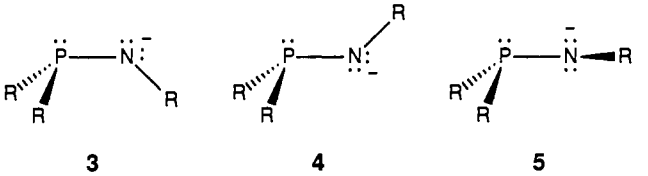

3 **4** **5**

(8) Trinquier, G. *J. Am. Chem. Soc.* **1986**, *108*, 568.
(9) Kutzelnigg, W. *Angew. Chem., Int. Ed. Engl.* **1984**, *23*, 272.
(10) (a) Schoeller, W. W.; Busch, T.; Niecke, E. *Chem. Ber.* **1990**, *123*, 1653. (b) Schoeller, W. W.; Busch, T.; Haug, W. *Phosphorus, Sulfur Silicon* **1990**, *49*, 285.
(11) Dupuis, M. *MOTECC89*; IBM Corp., Center for Scientific and Engineering Computations: Kingston, NY 12401, 1989.
(12) Durand, Ph.; Barthelat, J.-C. *Theor. Chim. Acta* **1975**, *38*, 283.

Table 3. Diagonal f Matrix Elements (mdyn/Å)

		f_{PN}	f_{PH}		f_{PF}		f_{NH}	f_{NF}	f_{HPN}		f_{FPN}		f_{PNH}	f_{PNF}	f_{XPNZ}	f_{YPNZ}
H_2P–NH^-	TS	4.67	2.85	2.70			7.59		1.09	1.04			0.48		0.70	0.70
	trans	5.07	2.88				7.45		1.08				0.70		0.85	
	cis	5.23	2.64				7.29		1.09				0.61		0.81	
HFP–NH^-	TS2	5.89	2.43		3.60		7.60		1.14		1.58		0.33		1.05	0.96
	TS1	6.27	2.59		2.95		7.90		1.22		1.35		0.32		1.00	0.93
	trans	6.56	3.22		2.59		7.53		1.19		1.16		0.64		1.05	1.16
	cis	6.73	2.77		2.60		7.40		1.20		1.24		0.58		1.10	1.11
H_2P–NF^-	TS	3.66	2.99	3.38				2.97	0.98	0.94				1.31	0.69	0.70
	trans	4.39	3.35	2.85				2.89	0.95	1.00				1.38	0.86	0.84
	cis	4.90	3.13					2.70	0.98					1.29	0.85	
F_2P–NH^-	TS	7.42			3.41	3.00	7.95				1.63	1.48	0.26		1.16	1.17
	trans	7.48			3.53		7.68				1.56		0.53		1.69	
	cis	7.77			3.10		7.58				1.51		0.45		1.57	
HFP–NF^-	TS2	4.53	3.15		3.83			3.08	1.09		1.36			1.04	1.00	1.01
	TS1	4.18	2.78		4.18			3.93	1.08		1.52			1.18	0.96	0.92
	trans	5.93	3.49		2.95			3.38	1.08		1.10			1.65	1.17	1.03
	cis	6.19	3.37		3.23			3.32	1.06		1.12			1.32	1.13	1.12
F_2P–NF^-	TS	5.46			4.26	3.59		4.26			1.73	1.42		1.13	1.20	1.08
	trans	6.20			3.49	4.47		3.88			1.67	1.28		1.21	1.53	1.81
	cis	6.71			3.95			4.24			1.46			1.07	1.68	

Table 4. Harmonic Vibrational Frequencies (cm^{-1})

	H_2P–NH^-		FHP–NH^-		H_2P–NF^-		F_2P–NH^-		FHP–NF^-		F_2P–NF^-	
	cis	trans	cis	trans	cis	trans	cis	trans	cis	trans	cis	trans
1	542	299	335	343	350	136	291	207	171	184	140	103
2	904	896	598	555	373	364	374	383	354	354	209	255
3	911	925	621	621	673	689	457	465	444	390	406	358
4	922	954	912	909	884	869	600	488	660	644	424	374
5	1134	1179	1030	1036	904	923	628	688	739	741	594	485
6	1246	1269	1078	1096	994	956	700	739	957	937	715	700
7	2116	2214	1139	1172	1273	1243	929	998	1064	1058	759	801
8	2166	2263	2196	2366	2315	2226	1153	1111	1098	1093	822	806
9	3629	3668	3656	3687	2348	2414	3698	3724	2421	2462	1149	1089

Table 5. Net Atomic Charges

		P	N	H(P)		F(P)		H(N)	F(N)
H_2P–NH^-	TS	0.19	−1.02	−0.20	−0.14			0.16	
	trans	0.10	−0.97	−0.15				0.16	
	cis	0.21	−0.98	−0.20				0.16	
HFP–NH^-	TS2	0.34	−0.99	−0.20		−0.31		0.17	
	TS1	0.42	−1.03	−0.15		−0.45		0.20	
	trans	0.16	−0.91	−0.09		−0.31		0.15	
	cis	0.38	−0.95	−0.19		−0.42		0.18	
H_2P–NF^-	TS	0.13	−0.57	−0.08	−0.12				−0.36
	trans	0.15	−0.60	−0.15	−0.09				−0.31
	cis	0.09	−0.52	−0.11					−0.35
F_2P–NH^-	TS	0.60	−0.98			−0.45	−0.34	0.17	
	trans	0.60	−0.95			−0.40		0.15	
	cis	0.57	−0.89			−0.42		0.17	
HFP–NF^-	TS2	0.38	−0.61	−0.07		−0.36			−0.34
	TS1	0.42	−0.58	−0.13		−0.36			−0.35
	trans	0.22	−0.53	−0.05		−0.32			−0.32
	cis	0.24	−0.52	−0.06		−0.35			−0.31
F_2P–NF^-	TS	0.67	−0.58			−0.40	−0.36		−0.34
	trans	0.69	−0.61			−0.38	−0.42		−0.27
	cis	0.70	−0.50			−0.44			−0.32

the transition state **5**. A local minimum corresponding to H_3PN^- is much higher in energy than the H_2PNH^- isomer (by 41 kcal/mol with respect to **3** at the SCF level). The corresponding geometrical parameters are given at the top of Table 1. The associated relative energies, force constants, harmonic vibrational frequencies, and net atomic charges are given in Tables 2–5, respectively. The more stable conformation is the cis form **3**, with the trans form **4** lying only 0.5 kcal/mol higher in energy. The barrier for interconverting the two forms however is 8 kcal/mol, which suggests that both forms **3** and **4** should durably coexist. Note that transition state **5** is a barrier to rotation around the P—N bond and not a barrier to inversion at N, as emphasized by the composition of the imaginary mode of **5** given in the first column of Table 6. This is in contrast with the cis/trans isomerization path of the parent phosphazene HP=NH, which occurs through a linearization of P—N—H with an activation barrier of about 15 kcal/mol.[3a] An estimate of the cost of nitrogen inversion in the anion H_2PNH^- has been made by calculating a form with a linear P—N—H moiety, while fixing all of the other geometrical parameters. By using either the cis or trans parameters, one obtains an upper limit of 27 kcal/mol at the SCF level, which should not be significantly decreased by further relaxing the remaining geometrical parameters. The reason for the large inversion barrier originates in the lone-pair repulsions at the nitrogen center. If the negative charge is largely located at nitrogen (as we shall see that it is) the $n_{sp^2} + n_p$ arrangement, **6**, is favored with respect to the $n_p + n_p$ one, **7**,as expected from

6 **7**

simple VSEPR arguments (cf. the linearization of H_2O or NH_2^-). On the other hand, the fact that cis/trans isomerization occurs via a *rotational* barrier in H_2P—NH^- and via an *inversion* barrier in HP=NH gives us insight into the nature of the PN bond. It is easier to rotate around a PN single bond than around a PN double bond, and it is easier to linearize a neutral nitrogen center =N– than an amide center –N–⁻. Obviously, when compared to the regular double bond of the phosphazene HP=NH, the PN bond in the phosphinoamide anion has little double-bond character. This supports the anionic amide form with the charge localized on nitrogen. Now, what about the rotational isomerization in neutral single-bonded aminophosphine H_2P—NH_2? A difficulty arises here because the interconversion of the two stable gauche forms, **8** and **10**, occurs through a bisected form bearing a planar arrangement of the PNH_2 group, **9**.[4] A rotational barrier

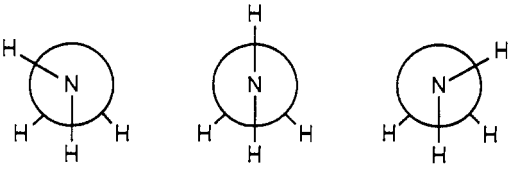

8 **9** **10**

Table 6. Composition (%) of the Imaginary Mode for the Saddle Points

			HFP–NH⁻				HFP–NF⁻		
		H_2P–NH^-	TS1	TS2	H_2P–NF^-	F_2P–NH^-	TS1	TS2	F_2P–NF^-
stretchings	P–N	–0.4	1.6	0.2	1.1	0.0	0.0	1.2	0.0
	P–H	–0.4	–0.9	–0.1	0.2		–0.1	–0.1	
		1.0			0.1				
	P–F		5.1	20.8		30.5	0.4	0.9	4.6
						–7.3			–4.5
	N–H	0.0	0.0	0.0		0.1			
	N–F				2.7		0.3	0.4	0.3
bendings	HPN	–1.1	–4.1	–3.7	0.5		0.1	0.0	
		5.5			0.0				
	FPN		2.0	6.2		16.7	0.0	–1.9	–3.9
						9.2			0.0
	PNH	1.4	–1.4	1.1		1.6			
	PNF				15.2		1.7	10.4	4.0
dihedrals	HPNH	40.2	15.7	5.0					
		50.1							
	FPNH		69.3	62.9		29.9			
						4.8			
	HPNF				43.0		4.0	0.5	
					37.4				
	FPNF						93.4	84.7	69.1
									13.6
	total	90.3	85.0	67.9	80.4	34.7	97.4	85.2	82.7

in a strict sense is difficult to define since there is no such saddle point. An estimate for the height of the rotational path can be given by the relative energy of the trans conformation. Calculated using our basis sets, such a form is located at 5 kcal/mol above the stable gauche form (both correlated and uncorrelated treatments lead to a roughly similar value, as in the present anion). When compared with the 7–8 kcal/mol obtained for the rotational barrier in H_2P—NH^-, this would suggest the PN linkage in the latter compound should have some (additional) multiple-bond character. Further insight is gained by comparing the equilibrium geometries, especially the P—N bond lengths, that have been calculated for these species.

The calculated PN bond length of the gauche form of aminophosphine is 1.71 Å (SCF DZP level). However, the bisected form, which is only 0.5 kcal/mol (SCF) or 0.9 kcal/mol (MP4) higher in energy than the gauche form, is more relevant since it exhibits C_s symmetry like the stable forms of H_2P—NH^-. This bisected form has a planar nitrogen and a p_π nitrogen lone pair that can delocalize into the phosphorus d_π orbital and the *antisymmetrical* combination of the empty σ_{P-H}* orbitals. This is why the PN bond length is a relatively short 1.69 Å, the P—H bond distances are slightly lengthened, and the phosphorus d orbital population is slightly increased (0.13 e^- vs 0.12 e^-) as compared to those of the gauche form. The cis form of the phosphinoamide may be thought of as arising from the deprotonation of the trans NH hydrogen of the bisected form of aminophosphine, while keeping the remaining C_s topology unchanged. The latter perspective suggests the following comparison:

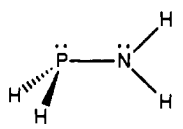

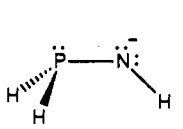

P-N (Å)	1.69	1.64
P-H	1.42	1.46
HPH (°)	94	99
NPH	102	110
PNH	126	113
dP	0.13	0.15

The PN bond in the model anion H_2PNH^- is significantly shortened (by 0.05 Å) with respect to the neutral aminophosphine H_2PNH_2. This is in agreement with the result obtained experimentally for $[Li(Ph_2PNPh)(OEt_2)]_2$ (1.672(2) Å).[6] For the cis and trans forms of H_2PNH^- the in-plane n_σ nitrogen lone pair can delocalize into the *symmetrical* combination of the empty σ_{P-H}* orbitals (note that the P—H bonds of H_2PNH^- are lengthened significantly) and to a lesser extent into a phosphorus d_π orbital. An analysis of the delocalized symmetry orbitals actually shows that a combination of the n(P) and n(N) occupied orbitals mixes with the PH antibonding orbitals. Is the shortened PN bond of H_2PNH^- consistent with the formally doubly bonded iminophosphide form H_2P^-=NH? We compare below the bond distance obtained for H_2PNH^- with typical singly and doubly bonded model systems calculated at the SCF level with similar basis sets:

H_2P-NH_2	gauche	1.71 Å single
H_2P-NH_2	bisected	1.69 Å
H_2P-NH^-	trans	1.65 Å
H_2P-NH^-	cis	1.64 Å
H_3P=NH		1.55 Å ylide
HP=NH		1.55 Å double

The PN bond in H_2P—NH^- is shorter than the corresponding typical single bond, but it is still larger (by about 0.1 Å) than a typical double bond. If one assigns some double-bond character to the bisected form of the aminophosphine and considers the gauche form to possess a regular PN single bond, the PN bond of the cis form of H_2PNH^- is 0.07 Å shorter than a single bond and 0.09 Å longer than a double bond, which places its distance at the approximate midpoint between the two limiting forms. If we take the bisected form as the prototype for a P—N single bond, then the shortening is only 0.05 Å, which would place the anion closer to the singly bonded system. Finally, the Mulliken analysis indicates that the negative charge is basically located on the nitrogen atom (see the net charges at the top of Table 5), which further favors the H_2P—NH^- phosphinoamide limiting form.

The small thermodynamic preference of the cis form over the trans form (confirmed at the MP4 level) is certainly due to the more favorable arrangement of the dipoles H_2^-—P^+ and N^-—H^+ in the former, which may also account for the difference in PN distances. The latter effect is enhanced by the large polarizability

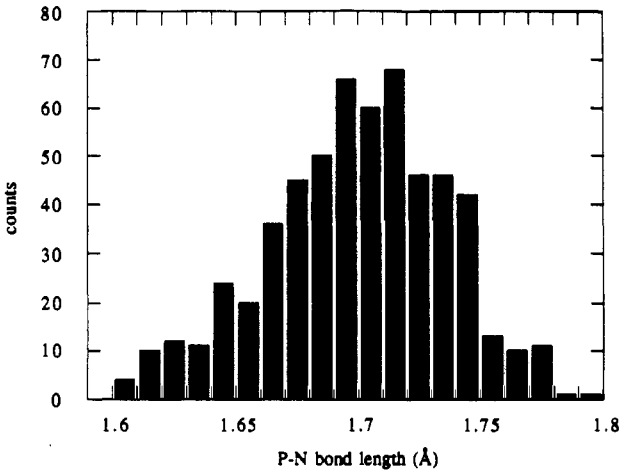

Figure 1. Histogram of the PN bond lengths for unconstrained aminophosphine-type systems encountered in the Cambridge Structural Database.

of the P—H bond. As illustrated by the atomic net charges that are listed at the top of Table 5, the P—H bond polarity increases in the cis form, allowing a more advantageous electrostatic interaction, whereas the net charges on N and H(N) are conserved in both conformers. Although this might not seem intuitive, the n_σ–n_σ lone pair repulsion is not larger in the cis form than in the trans form. This point has been discussed for the n_+n_- lone pair splitting in hydrazine and diphosphine.[4d]

The PN bond length in the Ph_2PNPh^- anions that form the complex $[Li(Ph_2PNPh)(OEt_2)]_2$ has been determined by single-crystal X-ray crystallography to be 1.672(2) Å.[6] We have searched the Cambridge Structural Database (CSD) for examples of unconstrained aminophosphine-type systems in order to assess the significance of the PN bond distance observed for $[Li(Ph_2PNPh)(OEt_2)]_2$. The results of this search, summarized in the histogram of Figure 1, yield a mean value of d_{P-N} = 1.70 Å (σ = 0.04 Å, 592 hits). According to this criterion, the PN bond in the complexed ion is about 0.03 Å shorter than a "normal" single bond. This result is roughly in line with the theoretical results of our model. A direct comparison of the PN bond lengths in the H_2PNH^- model and the real system (1.64 vs 1.67 Å) is complicated because of the interplay of a variety of factors. Disregarding the slight lengthening expected from a geometry optimized at a correlated level, the two main factors that influence the PN bond length in the real system are the substituent and complexation effects. Aromatic substitution at nitrogen should delocalize the negative charge and consequently lengthen the PN bond. Aromatic substitution at phosphorus, on the other hand, should delocalize any electron flow toward phosphorus and thereby shorten the PN bond. The latter substituent effect is however less straightforward than the former, so that PN bond lengthening could prevail. The complexation of the anion, be it N-η^1 or N,P-η^2, employs the nitrogen n_σ lone pair and will, therefore, partly destroy its delocalization toward phosphorus, thus inducing a PN bond lengthening as illustrated below.

Finally, the relative energies calculated for the H_2PNH^- model are in agreement with NMR data that suggest that Ph_2PNPh^- exists in two isomeric forms, close in energy, separated by an activation barrier of about 8 kcal/mol.[13]

(13) The ^{31}P spectrum of Ph_2PNPh^- in THF-d_8 consists of a singlet (38.0 ppm downfield from external H_3PO_4) at room temperature which splits into two singlets of approximately equally area (24.0 and 43.3 ppm) upon cooling the sample to −100 °C. The latter behavior indicates a dynamic process is being frozen out. The barrier to activation of the dynamic process was found to be 7.5 kcal at −83 °C (the coalescence temperature). Since the difference in chemical shifts (3860 Hz) is much greater than typical ^7Li–^{31}P coupling constants (~50 Hz), we conclude that the resonances are due to two phosphorus species that fortuitously exist in approximately equal abundance. The dynamic process may be hindered rotation about the P–N bond.

In order to assess the influence of complexation of the anion on its geometry and to understand the structural features observed for the $[Li(Ph_2PNPh)(OEt_2)]_2$ complex, a model complex $[Li(H_2PNH)]_2$ (**11**)was explored theoretically.[14] Besides the PN bond

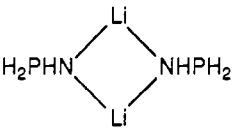

11

length change associated with complexation, we are particularly interested in the P···Li interaction observed in the solid-state structure of the real system. The model complex **11** is globally neutral and is made up of 2 H_2PNH^- + 2 Li^+, which are expected to keep their ionic nature in the complex and therefore bind largely through electrostatic interactions. The complex was first examined with its geometry constrained to C_{2h} symmetry (i.e. implying a planar four-membered ring and a trans arrangement of the N–PH_2 groups) with each H_2PNH ligand being in a cis conformation. This geometry is not far from the experimental one, of lower C_i symmetry and should permit symmetrical P···Li interactions. We started with a short P–Li distance (2.68 Å, as observed in the real complex). Optimized at the SCF level, the system relaxes toward an arrangement in which the PH_2 groups are tilted outside and far away from the Li^+ ions, with NNP angles of 123° and P–Li distances of 3.11 Å (**12**). We next tried

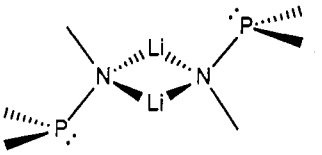

12

to detect a minimum corresponding to a C_i-distorted structure, with the $[LiPN]_2$ moiety being assigned its experimental geometry. The geometry once again relaxed to the C_{2h} one. All other attempts to capture any geometric form with a short P···Li contact led to the same minimum. Unless we have missed a shallow local minimum, it would appear that the model anion H_2PNH^- only binds lithium in an η^1 fashion. We have calculated the energy change that occurs when the H_2PNH^- groups in **12** are tilted about the nitrogen atom so as to bring the phosphorus atoms closer to the lithium ions. The corresponding energy curve is monotonously repulsive, without any shoulders in the region of possible Li···P interaction. For an NNP angle of 96°, corresponding to the short P–Li contact of 2.68 Å observed experimentally, the energy loss is 9 kcal/mol with respect to **12**, which seems difficult to counterbalance by the relaxation of all other geometrical parameters. We therefore suggest there exists a single minimum. The SCF-calculated geometrical parameters for the model complex are listed in Table 7. The corresponding vibrational frequencies are given in Table 8, together with their assignments and infrared intensities.

The geometry about the nitrogen atoms of **12** allows optimal interaction of the two nitrogen lone pairs with the two lithium ions, these lone pairs being described either as two sp^3 localized hybrids or with the $n_\sigma + p_\pi$ set which takes into account the local symmetry of the ligand. The existence of such a deep minimum would suggest for our model a point-charge-driven arrangement. This is in agreement with a negative charge mainly localized on

(14) The coordination chemistry of an iminophosphide/phosphinoamide anion bound to zirconium was reported recently. Spectroscopic results suggest the ion can bind through both the phosphorus and nitrogen atoms; however, no X-ray structural data are available: Igau, A.; Dufour, N.; Mathieu, A.; Majoral, J.-P. *Angew. Chem., Int. Ed. Engl.* **1993**, *32*, 95.

Table 7. Calculated Geometrical Parameters for C_{2h} $(H_2PNHLi)_2$ (Å, deg)

ligand		ring	
P–N	1.695	N–Li	1.959
P–H	1.423	LiNLi	72.6
N–H	1.013	NLiN	107.4
HPH	93.2	NNP	123.2
PNH	111.9	NNH	124.9
NPH	105.5	PNLi	116.2
		HNLi	117.4

Table 8. Harmonic Vibrational Frequencies for $(H_2PNHLi)_2$ (cm^{-1})

sym	freq	IR intens	main assignment
$1b_u$	69	0.3	N–PH_2 rocking + ring puckering
$1a_u$	77	0.3	N–PH_2 wagging
$1a_g$	104		N–PH_2 scissoring + PN str
$1b_g$	141		N–PH_2 twisting
$2a_u$	214	0.5	N–PH_2 wagging
$2b_g$	221		PN torsion
$2b_u$	307	2.6	ring puckering + PN str
$2a_g$	338		ring in–plane bending + PN str
$3a_u$	451	3.1	N–PH_2 wagging
$3b_g$	540		LiN str
$3a_g$	569		ring in–plane bending + PN str
$3b_u$	616	4.0	
$4a_u$	706	5.7	
$4b_g$	716		
$4a_g$	882		PN str
$4b_u$	887	13.5	PN str
$5a_g$	958		
$5a_u$	973	2.5	
$5b_g$	974		
$5b_u$	976	3.6	
$6a_g$	1237		
$6b_u$	1237	4.2	
$7b_u$	1271	0.2	
$7a_g$	1272		
$6b_g$	2428		PH str
$6a_u$	2428	10.5	PH str
$8b_u$	2440	11.6	PH str
$8a_g$	2442		PH str
$9a_g$	3684		NH str
$9b_u$	3687	0.1	NH str

nitrogen in the isolated anion. The disagreement with the η^2 binding experimentally found for Ph_2PNPh^- may be due in part to more delocalization of the negative charge in the real system. Also, potential crystal packing effects cannot be ignored, although we have not identified any particular such interaction that would account for the observed η^2 interaction of the anions with the cations.

As expected, the complete involvement of the nitrogen lone pairs in complexation with the lithium ions prevents their delocalization into the PR_2 group, which induces a lengthening of the PN bond. Remarkably, the PN bond length found for $[Li(H_2PNH)]_2$ is similar to that in the single-bonded bisected aminophosphine. In fact, most of the geometrical properties of the N–PH_2 group in the complex are similar to those of the neutral bisected aminophosphine:

	H_2PNH^-	$[Li(H_2PNH)]_2$	H_2PNH_2
P-N (Å)	1.64	1.69	1.69
P-H (Å)	1.46	1.42	1.42
HPH (°)	89	93	94

The charge distribution in the complex is the result of two effects: (1) some electron delocalization from nitrogen toward lithium (which is responsible for chemical bonding) and (2) maximization of charge contrast over the Li_2N_2 rhombus. The Mulliken population analysis indicates that each lithium ion has received 0.19 e^- from the anionic ligand. The net charge on nitrogen is *increased* to –1.07. It is therefore the H and P atoms of the ligands that lose electron density to the benefit of the Li and N centers. This partitioning clearly illustrates the global migration of electron density from the extracyclic groups toward the four-membered ring. The complex is mainly bound through electrostatic interactions between the charges of alternating signs borne by these four centers. Since these charges are of the magnitude of point charges, the binding energy of the complex with respect to 2 Li^+ + 2 H_2PNH^- is expected to be large. It is calculated to be 391 kcal/mol at the SCF level, which incidentally is close to the energy that is required to deprotonate H_2PNH_2 (C_1) to give *cis*-H_2PNH^- (SCF, 394 kcal/mol; MP4, 389 kcal/mol).

The shape of the Li_2N_2 rhombus in the model complex is similar to that in the real complex except for the N–Li distance, which is found to be 0.06 Å shorter than that found in the real complex. Again, linkage of the ligand and lithium ions in the latter complex occurs through both nitrogen and phosphorus. The ligand only binds through the nitrogen atoms in our model system. This should at least partially account for the shorter Li–N bonds calculated for the model system, another possible origin being related to the absence of correlation in our geometry optimization step. A search of the Cambridge Structural Database (CSD) for systems that include N_2Li_2 four-membered rings led to an even larger value for Li–N (d = 2.06 Å, σ = 0.06 Å, 142 hits), while the shape of the rhombus seems to be rather constant, as follows:

	CSD mean	$[Li(Ph_2PNPh)(OEt_2)]_2$	$[Li(H_2PNH)]_2$
Li-N (Å)	2.06	2.02	1.96
N-Li-N (°)	104	105	107
Li-N-Li (°)	74	75	73

The harmonic vibrational frequencies given in Table 8 may be used for the assignment of some infrared frequencies. We find in particular a strong band at 887 cm^{-1} that corresponds at 80% to a PN stretching mode. Applying a scaling factor of 0.9 would locate this band around 800 cm^{-1}. Notice also a set of four collective modes at 69–141 cm^{-1} corresponding to motions of the N–PH_2 groups and deformations of the ring. This suggests that the complex is not rigid even at temperatures as low as ca. –70 °C.

Fluoro Derivatives R_2PNR^- (R = H, F)

The optimized geometries corresponding to the stationary points for the five possible fluoro derivatives are given in Table 1. The corresponding relative energies, force constants, vibrational frequencies, and net atomic charges are listed in Tables 2–5, respectively. Again, two stable conformations, cis and trans, are found for the fluoro derivatives of the parent model compound. For the derivatives that bear a single fluorine substituent at phosphorus, $HFPNH^-$ and $HFPNF^-$, these two minima no longer exhibit C_s symmetry. For the cis conformers, the respective dihedral angles between NR and the bisect of the HPF angle are 15 and 18° in the direction of PH (**13**). For the trans conformers,

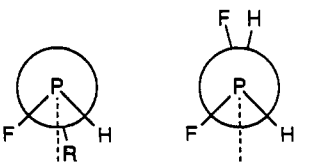

13 **14**

the respective deviations, 17 and 35°, are in the opposite sense for the two derivatives (**14**). Moreover, for these unsymmetrical derivatives, two rotational transition states are possible: TS1, **15**; TS2, **16**. Such structures were actually found to be saddle points of index 1 and are addressed in the tables.

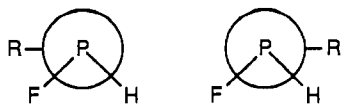

TS1 TS2

15 16

The trans forms of H_2PNF^- and F_2PNF^- are unexpectedly slightly distorted from C_s symmetry. This distortion corresponds to rotations about the PN bond of 21 and 26° for the two compounds, respectively. The C_s trans form is the saddle point that relates these two equivalent C_1 forms. It lies only 0.1 and 0.4 kcal/mol, respectively, above the corresponding C_1 conformers (SCF and MP4 levels give the same relative energies). The barrier associated with the double well for H_2PNF^- vanishes when the zero-point energies (ZPE) are taken into account. The double well observed for F_2PNF^- would survive the ZPE correction, but it is reduced to 0.2 kcal/mol. We are not convinced that the barriers are real since the geometries were determined at the SCF level only and refinement at a correlated level could compensate for such a small energy difference. We suggest that these trans forms have mean C_s structures that exhibit large-amplitude motion with respect to such deformations.

The relative energies (Table 2) indicate that the cis and trans forms of $HFPNH^-$ and $HFPNF^-$ remain nearly energy degenerate, with correlation effects even favoring the trans form for the former. For F_2PNH^- and F_2PNF^-, the trans form lies 4 kcal/mol above the cis form. For H_2PNF^-, the difference is 6 kcal/mol. The origin of these energy differences should be traced to an interplay among bond polarities, bond polarizabilities, and overlap factors.

The transition states relating the two stable conformations of the derivatives always have energy barriers that are larger than that for the parent compound. They range from 10 to 22 kcal/mol. This could suggest some double-bond character for the PN bond, but we shall see below that this is not true for H_2PNF^-. So, the origin of these differences in the rotational barriers should be traced to an interplay of repulsive and overlap effects, and also to the following point. If we examine the internal coordinates involved in the imaginary mode (Table 6), one can see that in most cases the main motion involved is actually the rotation about PN, as measured by the sum of the dihedral coordinates. This sum ranges between 80% and 97% (cf. last line of Table 6) except for F_2PNH^-, where it is only 35%, and $HFPNH^-$ (TS2), where it is 68%. In these cases the imaginary mode involves a significant contribution of PF stretching and FPN bending. The saddle point for F_2PNH^- would actually correspond to a mixing of PF dissociation, NPF inversion, and PN torsion. The barrier associated with this transition state happens to be the lowest one of all the fluoro derivatives.

Substituent effects on the PN bond strength in phosphazenes RP=NR′ have been discussed by Schoeller *et al.*[10] They showed that a σ-acceptor substituent, such as the fluorine atom, strengthens the PN bond when it is at phosphorus, whereas it weakens it when it is at nitrogen, as reflected by the corresponding calculated PN bond shortening or lengthening, respectively. A similar trend was also illustrated with chlorine-substituted aminophosphines.[4c] The PN bond strengthening upon fluorine substitution at phosphorus in aminophosphine has been evidenced and further interpreted by Reed and Schleyer in terms of negative hyperconjugation or generalized anomeric effects.[4g] From our calculated PN bond lengths and force constants given in Tables 1 and 3, the trend is confirmed in our anionic systems. For the derivatives that are substituted at a single center, the expected ordering for decreasing PN bond strengths is obtained: F_2PNH^- > $HFPNH^-$ > H_2PNH^- > H_2PNF^-. The ions $HFPNF^-$ and F_2PNF^- that are substituted at nitrogen and phosphorus are not easily placed *a priori* in this scale. Substitution at phosphorus

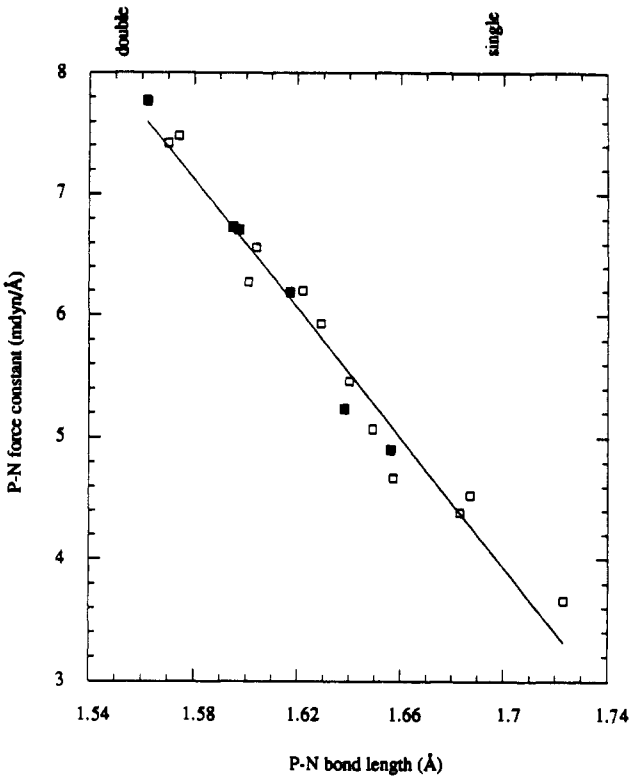

Figure 2. PN force constants versus PN bond lengths for the anions studied. Solid squares correspond to the cis conformers.

seems to prevail since both have stronger PN bonds than the parent compound. The following ordering of decreasing PN strength is therefore obtained: F_2PNH^- > $HFPNH^-$ > F_2PNF^- > $HFPNF^-$ > H_2PNH^- > H_2PNF^-. A good linear dependence (r = 0.98) is found when the force constants are plotted against the PN bond lengths for all of the conformers and saddle points (Figure 2). The full scale roughly ranges from a typical PN double-bond length (1.55 Å) to a typical single-bond length (1.70 Å), which suggests the plastic nature of the PN bond. According to this criterion, the derivative F_2PNH^- can be seen as a formal P=N double-bonded system. Bond indexes calculated using Mayer's definitions[15] roughly reflect the above ordering, with some differences originating from the ambivalence of fluorine, both as a σ-withdrawing and a π-donating substituent. The bond indexes in fact also depend on the nature of fluorine substitution. The following ordering again ranges between single and double PN bond lengths, with F_2PNH^- again being closer to a formally double-bonded derivative:

H_2P-NH_2 (C_s)	0.63
H_2P-NH^-	0.76
H_2P-NF^-	0.88
HFP-NH^-	1.04
HFP-NF^-	1.16
F_2P-NF^-	1.33
F_2P-NH^-	1.40
HP=NH	1.81

The arguments developed by Schoeller to account for the substituent effects in iminophosphanes[10] can also be applied to the phosphinoamide/iminophosphide anions. A σ-attractor such as fluorine tends to confer ionic character to the F—X bond,

(15) Mayer, I. *Chem. Phys. Lett.* **1983**, *97*, 271. Villar, H. O.; Dupuis, M. *Chem. Phys. Lett.* **1987**, *142*, 59.

Scheme 1

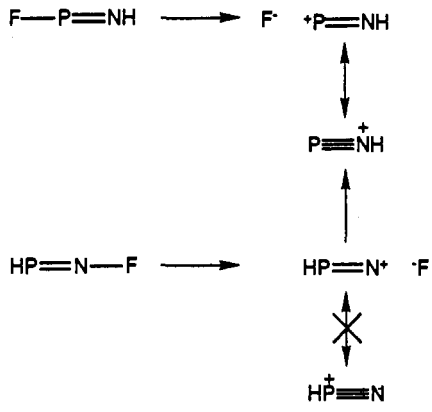

Scheme 2

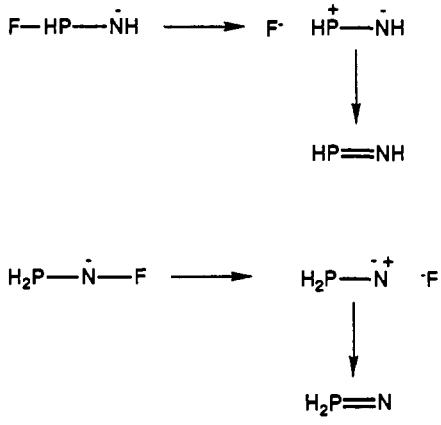

which corresponds in valence-bond language to an enhanced weight of the ionic determinant associated with the configuration $F^- {}^+X$. This effect is all the more stabilizing when (1) the electronegativity difference between F and X is large and (2) the X^+ moiety is stabilized with respect to other competing configurations. In the model iminophosphane HP=NH, fluorine substitution at phosphorus induces a $^+$P=NH moiety, whereas fluorine substitution at nitrogen induces a HP=N$^+$ moiety. Not only is the $^+$P=NH fragment stabilized by resonance, but it is also the only minimum on the potential surface (HP=N$^+$ is not even a local minimum).[10] This explains why the P=N bond is strengthened in FP=NH whereas it is weakened in HP=NF (Scheme 1).

In the same way, fluorine substitution at phosphorus in the model phosphinoamide anion H_2P—NH^- will yield the HP=NH moiety while fluorine substitution at nitrogen will yield the H_2P=N moiety (Scheme 2). Although the latter fragment would exhibit a somewhat higher bond order than the former,[3a] it happens to be much less stable (by 41 kcal/mol), so that again the fluorine substitution at phosphorus strengthens the PN bond while that at nitrogen does not.

Table 9. Relative Energies between Isomers (kcal/mol)

		SCF	MP4	from BE[a]
H_2FPN^-	H_2P–NF^-	70.4	67.5	67.0
	HFP–NH^-	0.0	0.0	0.0
F_2HPN^-	HFP–NF^-	80.8	75.4	67.0
	F_2P–NH^-	0.0	0.0	0.0

[a] Evaluation from simple mean bond energy differences.

A more straightforward explanation is possible for the relative stabilities of isomers with the same formula, namely $HFPNH^-$ and H_2PNF^- on one hand and F_2PNH^- and $HFPNF^-$ on the other. From the standard mean bond energies for P–H, P–F, N–H, and N–F (e.g. 78, 119, 93, and 67 kcal/mol, respectively),[16] one may predict that the isomer with the highest fluorine substitution at phosphorus should be stabilized by roughly the difference in bond energy: (119 – 78) – (67 – 93) = 67 kcal/mol. It can be seen in Table 9 that this is indeed close to our calculated relative energies.

The main results that emerge from this theoretical study may be summarized as follows: (1) The parent anion H_2PNH^- has a shortened PN bond length, and it exhibits two possible conformations, cis and trans, that are nearly degenerate in energy and are separated by a significant energy barrier. (2) Its structure is basically that of a phosphinoamide rather than that of a iminophosphide anion. (3) A model complex of two such anions with two lithium cations does not exhibit the short P–Li contact found experimentally in $[Li(Ph_2PNPh)(OEt_2)]_2$, suggesting the phenyl groups are largely involved in delocalizing the negative charge. (4) Fluorine substitution may enhance the cis–trans energy difference (up to 6 kcal/mol for H_2PNF^-) as well as the corresponding rotational barrier (up to 22 kcal/mol for $HFPNF^-$). (5) As observed in phosphazenes, fluorine substitution at phosphorus strengthens the PN bond while fluorine substitution at nitrogen weakens it. This confers on F_2PNH^- a structure that is formally close to the iminophosphide form.

Acknowledgment. We thank Drs. J. Aussoleil and A. Gourdon for their assistance with the CSD. M.T.A. is grateful to the University of Oklahoma Research Council for a Junior Faculty Summer Research Fellowship and the Halliburton Faculty Development Program for their financial support.

(16) Purcell, K. F.; Kotz, J. C. *Inorganic Chemistry*; Saunders: Philadelphia, PA, 1977; p 270.